



HAL
open science

Dynamic bedrock channel width during knickpoint retreat enhances undercutting of coupled hillslopes

Edwin Baynes, Dimitri Lague, Philippe Steer, Philippe Davy

► To cite this version:

Edwin Baynes, Dimitri Lague, Philippe Steer, Philippe Davy. Dynamic bedrock channel width during knickpoint retreat enhances undercutting of coupled hillslopes. *Earth Surface Processes and Landforms*, 2022, 47 (15), pp.3629-3640. 10.1002/esp.5477 . insu-03779168

HAL Id: insu-03779168

<https://insu.hal.science/insu-03779168>

Submitted on 16 Sep 2022

HAL is a multi-disciplinary open access archive for the deposit and dissemination of scientific research documents, whether they are published or not. The documents may come from teaching and research institutions in France or abroad, or from public or private research centers.

L'archive ouverte pluridisciplinaire **HAL**, est destinée au dépôt et à la diffusion de documents scientifiques de niveau recherche, publiés ou non, émanant des établissements d'enseignement et de recherche français ou étrangers, des laboratoires publics ou privés.



Distributed under a Creative Commons Attribution 4.0 International License

Baynes Edwin R C (Orcid ID: 0000-0002-8666-7628)

Dynamic bedrock channel width during knickpoint retreat enhances undercutting of coupled hillslopes

1. Geography and Environment, Loughborough University, Loughborough, UK
2. Université de Rennes, CNRS, Géosciences Rennes – UMR 6118, Rennes 35000, France

* Corresponding author email address: e.baynes@lboro.ac.uk

Acknowledgments

We thank Jean-Jacques Kermarrec for his assistance with the laboratory experiments. We also thank two anonymous reviewers for their comments which improved a previous version of this manuscript. The research was funded by the European Union's Horizon 2020 research and innovation programme through a Marie Skłodowska-Curie Actions Individual Fellowship (no. 703230 to EB), and the European Research Council (ERC) under the European Union's Horizon 2020 research and innovation programme (grant agreement No 803721 to PS).

Author contributions

EB, DL and PS designed the study. PD developed the numerical hydrodynamic model. EB performed the laboratory experiments and numerical simulations. All authors contributed to the data analysis and interpretation of the results. EB wrote the paper with input from all the authors.

Data Availability Statement:

This article has been accepted for publication and undergone full peer review but has not been through the copyediting, typesetting, pagination and proofreading process which may lead to differences between this version and the Version of Record. Please cite this article as doi: 10.1002/esp.5477

The data that support the findings of this study are available from the corresponding author upon reasonable request.

Abstract

Mountain landscapes respond to transient tectonic and climate forcing through a bottom-up response of enhanced bedrock river incision that undermines adjoining hillslopes, thus propagating the signal from the valley bottom to the valley ridges. As a result, understanding the mechanisms that set the pace and pattern of bedrock river incision is a critical first step for predicting the wider mechanisms of landscape evolution. Typically, the focus has been on the impact of channel bed lowering by the upstream migration of knickpoints on the angle, length and relief of adjoining hillslopes with limited attention on the role of dynamic channel width. Here, we present a suite of physical model experiments that show the direct impact of knickpoint retreat on the reach-scale channel width, across a range of flow discharges (8.3 to $50 \text{ cm}^3 \text{ s}^{-1}$) and two sediment discharges (0 and $0.00666 \text{ g cm}^{-3}$). During knickpoint retreat, the channel width narrows to as little as 10% of the equilibrium channel width while the bed shear stress is $>100\%$ higher immediately upstream of a knickpoint compared to equilibrium conditions. We show that only a fraction of the channel narrowing can be explained by existing hydraulic theory. Following the passage of a knickpoint, the channel width returns to equilibrium through lateral erosion and widening. For the tested knickpoint height, we demonstrate the lateral adjustment process can be more significant for hillslope stability than the bed elevation change, highlighting the importance of considering both vertical and lateral incision in landscape evolution models. It is therefore important to understand the key processes that drive the migration of knickpoints, as the localised channel geometry response has ongoing implications for the stability of adjoining hillslopes and the supply of sediment to the channel network and export from landscapes onto neighbouring depositional plains.

Keywords: Bedrock river, Channel width, Knickpoint, Hillslope, Analogue experiments, Lateral erosion, Cohesive substrate

1. Introduction

The dynamic adjustment of bedrock river channels to transient forcing controls the mechanism and pace of wider landscape evolution (e.g., Burbank et al., 1996; Duvall et al., 2004; Whittaker et al., 2007; Lague, 2014; DiBiase et al., 2015; Yanites, 2018), with increasing recognition that landscape-scale studies require an understanding of the coupling of in-channel and hillslope processes (e.g., Hurst et al., 2019). A common manifestation of this phenomenon is the bottom-up landscape adjustment to changes in external forcing (e.g., tectonic uplift rate or base level fall) through the upstream migration of knickpoints often in the form of waterfalls or channel reaches with a heightened bed slope. At a knickpoint, the channel bed elevation drops relatively suddenly so as it migrates upstream the signal of base level fall (e.g., increased uplift rate) is transferred to the adjoining hillslopes leading to their steepening, lengthening, increased relief (Gallen et al., 2011; Hurst et al. 2013; Grieve et al. 2015) and a shift in the pattern of basin hypsometry (Gallen et al., 2011). As a result, hillslopes can become destabilised and contribute more sediment to the fluvial system (Attal et al., 2015) due to increased hillslope potential energy leading to enhanced mass-wasting events such as landsliding, rockfalls or debris flows (Korup and Schlunegger, 2007; Reinhardt et al., 2007; Gallen et al., 2011; Mackey et al. 2014; Golly et al., 2017). Therefore, the physical processes that control the dynamic adjustment of bedrock channel morphology during knickpoint retreat have important implications for adjoining hillslopes and wider landscape evolution over short and long timescales.

The vertical adjustment of channel bed elevation during knickpoint retreat and its role in controlling downstream hillslope morphology, including hillslope destabilisation, is well known and has been identified extensively in multiple field settings (e.g., Swiss Alps; Korup and Schlunegger, 2007; Southern Spain; Reinhardt et al., 2007; Southern Appalachians; Gallen et al., 2011; Kua'i, Hawai'i; Mackey et al. 2014;

California; Hurst et al., 2019) as well as in laboratory experiments (e.g., Hasbergen and Paola, 2000; Bigi et al., 2006; de Lavaissiere et al., 2021). In contrast, the importance of processes that govern lateral adjustment of bedrock channel geometry has received relatively little attention compared to vertical incision processes (e.g., Wobus et al., 2006; Finnegan et al., 2007; Turowski et al., 2009; Yanites and Tucker, 2010; Cook et al., 2013; Whitbread et al., 2015; Turowski, 2018; Baynes et al., 2020; Li et al., 2020), and has primarily focused on the role of sediment availability and transport (e.g., the tools and cover effects).

Channel morphology is expected to change at, and upstream of, waterfalls/knickpoints due to variability associated with the flow hydraulics (e.g., Haviv et al., 2006). Rouse (1936) performed a series of experiments to demonstrate the presence of a flow-acceleration zone upstream of a freefall lip (i.e., the brink of waterfall), as a consequence of a pressure gradient induced by the shift from hydrostatic to atmospheric pressure dominating (Haviv et al., 2006; Flores-Cervantes et al., 2006; Lapotre and Lamb, 2015). The magnitude of flow acceleration is a function of the Froude number upstream of the waterfall (Rouse, 1936) and impacts the flow velocity, water depth and shear stress acting on the bed over a distance of two to four times the normal flow depth (Stein and Julien, 1993), under the assumption of a fixed channel width (Haviv et al., 2006):

$$\frac{\tau_{lip}}{\tau_{upstream}} = \left(1 + \frac{\varepsilon}{Fr_{upstream}^2}\right)^2 \quad (\text{Eqn 1})$$

Where τ_{lip} is the shear stress at the waterfall lip, $\tau_{upstream}$ is the shear stress upstream of the flow acceleration zone (i.e., at 'normal' conditions), $Fr_{upstream}$ is the Froude number upstream of the flow acceleration zone and ε is an empirical constant determined experimentally by Rouse (1936), with a value of 0.4. Haviv et al. (2006) also demonstrated the impact of the flow acceleration zone on the upstream channel slope, with the formation of an oversteepened reach possible when the rate of erosion at the waterfall face is lower than the rate of erosion at the waterfall lip. While the hydraulic theory above predicts a zone of higher shear stress and flow velocity acceleration is primarily a phenomenon of vertical waterfalls, it was also documented experimentally by Gardner (1983) and Baynes et al. (2018a) for break-in-slope knickpoints. It is logical, if the flow acceleration upstream of a waterfall is

sufficient to enhance erosion to the point of producing a long oversteepened convex reach upstream (e.g., Haviv et al., 2006), that the channel morphology and typical scaling of the channel width and depth would also be affected. For example, due to the principle of conservation of mass and the relationship between hydraulic radius, slope, and flow velocity in Manning's equation, it is possible that channels can narrow with increasing channel slope (Finnegan et al., 2005). Such observations have been made for natural channels in convex knickzones, with channel widths reported to be narrower than would be expected under typical bedrock river hydraulic scaling (Lague, 2014) in the French Alps (Valla et al., 2010), Turkey (Whittaker and Boulton, 2012), the Italian Apennines (Whittaker et al., 2007) and in Taiwan, where the Da'an river channel narrowed substantially during a period of rapid knickpoint retreat after the Chi-Chi earthquake (Cook et al., 2013). Despite these observations, and the hydraulic theory that predicts flow acceleration zones upstream of knickpoints, there remains an incomplete understanding of channel width variation in transiently adjusting reaches of bedrock channels (i.e., knickpoints and knickzones) and the possible implications for the stability of adjoining hillslopes.

In this paper, we investigate the role of lateral adjustment of channel geometry during transient knickpoint migration for the first time, and present a set of systematic analogue flume experiments to document the extent to which channel width adjustment is a significant process within the transient response of channels to changes in external forcing.

2. Physical Modelling of transient channels

2.1 Flume setup and experimental conditions

Due to the slow rates of knickpoint migration and bedrock channel adjustment in the natural environment, field observations often provide important insights into the response of the bedrock channel geometry to external forcing (e.g., Whittaker et al., 2007) and knickpoint formation processes (e.g., Groh and Scheingross, 2021) but lack insights into the temporal dynamics of these processes. We therefore performed a suite of analogue physical modelling experiments where the spatial and temporal scales of bedrock erosion processes are reduced (Paola et al., 2009). The laboratory modelling approach allows a systematic investigation of channel width evolution during knickpoint retreat, and whether input parameters (water and sediment

discharge; Q and Q_s , respectively) have an impact on the magnitude and rate of any channel width adjustment.

Experiments were performed using the 80 x 30 cm Bedrock River Experimental Incision Tank at the Université de Rennes. The flume setup has been described in detail previously in Baynes et al. (2018a; 2018b; 2020) and implements a 'similarity of process' analogue modelling approach whereby no formal scaling of the experiments with a particular natural location is sought. The experiments presented here do not, therefore, represent scaled experimental versions of any particular natural river, but the appropriate process representation within the flume allows the relative impact of the initial boundary conditions on the channel morphodynamics to be explored (Hooke, 1968; Paola et al., 2009; Baynes et al., 2018c). The scaling of width and slope of the experimental channels with discharge follows the patterns observed in natural channels (Baynes et al., 2018a), ensuring that the findings from the experimental channels are transferrable to the natural environment despite erosion being driven primarily by hydraulic shear rather than sediment impacts.

We used a cohesive mix of granular silica cement, spherical beads (ratio 3:1 granular silica to spherical beads, both 45 μm grain size) and water (18% of total mix volume) to represent a cohesive bedrock substrate in the experimental channels (Fig. 1). At the beginning of the experiments, we flowed water over the silica surface with a 2 cm initial base level fall to allow the channel to self-form an equilibrium geometry (width and slope) constrained within silica 'bedrock' banks (Fig. 1A;C). We performed 11 experiments (Table 1) at water discharges ranging from 8.33 $\text{cm}^3 \text{s}^{-1}$ to 50 $\text{cm}^3 \text{s}^{-1}$ (0.5 l min^{-1} to 3 l min^{-1}), with two scenarios of input sediment of coarse sand of 250 μm grain size: (i) $Q_s = 0$ grams of sediment per cm^3 of water (g cm^{-3}), (ii) $Q_s = 0.00666$ grams of sediment per cm^3 of water (g cm^{-3}). For each experiment, we triggered an upstream migrating knickpoint within the equilibrium channel by dropping the flume outlet plate by 3 cm instantaneously to replicate a sudden base level fall. As the knickpoint migrated upstream during the experiment, a green-laser terrestrial laser scanner (Leica ScanStation 2) collected high-resolution point clouds of the channel morphology at 2 minute intervals. The point clouds were converted into Digital Elevation Models with 2 mm horizontal resolution, and used as input data for the *Floodos* hydrodynamic numerical model (Davy et al. 2017) to generate water depth masks at each time interval. The *Floodos* generated water depth masks were

used to automatically extract the channel widths as well as calculate the bed shear stress during each time step of each experiment (see Baynes et al. 2018a; 2018b; 2020 for more details of the experimental procedure and coupling with the *Floodos* model).

To avoid any potential influence of the water inlet and outlet on the channel width, we removed the channel width data from the upper and lower 10 cm of the flume from any further analysis (Baynes et al., 2020). Observations of knickpoint location during the experiments were made through a combination of manual observations of the break in slope in the channel long profile and the location of an area of deeper water in a pool downstream (Fig. 1B;D). We used the width at the channel mid-point (i.e., 50% distance from the inlet to the outlet) as the reference location to extract the channel geometry characteristics for the knickpoints for the time period when the channel midpoint first experienced the knickpoint (i.e., when the oversteepened channel reaches the midpoint) through to the time when the knickpoint has fully migrated upstream (i.e., when the downstream limit of the pool is upstream of the midpoint). Therefore, the mean knickpoint width value in figure 2 encompasses all phases of a knickpoint, from lip to pool, as it migrates past the channel mid-point. We selected this approach for knickpoint channel width extraction to facilitate appropriate data extraction for knickpoints where the reach of active incision was relatively long (i.e., a steepened reach) or for a single vertical step undergoing parallel retreat.

2.2 Experimental results

2.2.1 Impact of transient incision on channel geometry

At equilibrium conditions before the base level was dropped by 3 cm, the width of the experimental channel increases with Q (Fig. 2A) following a power law (all experiments: $W_{Eq} = 11.9 Q^{0.52}$; $R^2 = 0.53$) consistent with typical natural bedrock channels (Lague, 2015). The experiments that had an additional input Q_s were wider ($W_{Eq} = 13.5 Q^{0.54}$) than those without an input Q_s ($W_{Eq} = 11.9 Q^{0.48}$), matching previous experimental results (Baynes et al. 2020). The channel width at the knickpoints at the channel mid-point are systematically narrower (all experiments: $W_{KP} = 4.74 Q^{0.58}$; $R^2 = 0.69$, $Q_s = 0.00666 \text{ g cm}^{-3}$ experiments: $W_{KP} = 3.7 Q^{0.67}$; $R^2 = 0.71$, $Q_s = 0 \text{ g cm}^{-3}$ experiments: $W_{KP} = 5.9 Q^{0.51}$; $R^2 = 0.96$) than the channel width at equilibrium conditions (Fig. 1;2A). The amount of narrowing of the channel at the

knickpoint compared to equilibrium conditions increases for higher Q , with the knickpoint at $50 \text{ cm}^3 \text{ s}^{-1}$ with $Q_s = 0.00666 \text{ g cm}^{-3}$ up to 100 mm narrower than the equilibrium channel (Fig. 2A). Importantly, however, the magnitude of channel narrowing at the knickpoints when normalised by the equilibrium channel width shows no relationship with Q (Fig. 2B). Knickpoints with $Q_s = 0.00666 \text{ g cm}^{-3}$ are proportionally narrower than their equilibrium conditions compared to the experiments with $Q_s = 0 \text{ g cm}^{-3}$, across the full range of Q (Fig. 2B). The value of bed shear stress follows the pattern observed in Baynes et al. (2018a) for a similar suite of experiments, with the shear stress at the lip of the knickpoints $\sim 2 \text{ Pa}$, greater than the equilibrium value $\sim 1 \text{ Pa}$, and showing no clear relationship with increasing Q (Fig. 2C). The bed shear stress in experiments where $Q_s = 0.00666 \text{ g cm}^{-3}$ is higher than the clear water flow experiments, following a similar pattern to the channel width where increased narrowing of the width leads to higher water depths for a given Q (Fig. 2D), and therefore a higher bed shear stress. The channel bed slope also varies between equilibrium conditions and reaches upstream of the knickpoints, with channels steepening locally during the phase of transient adjustment (i.e., at the knickpoints; Fig. 2E).

2.2.2 Temporal evolution of channel width during transient adjustment

2.2.2.1 Reach scale adjustment

Due to the reduced spatial scale and analogue processes at work in the flume experiments, the temporal evolution of the channel geometry is accelerated compared to natural bedrock systems. As a result, we are able to observe the coincident channel geometry adjustment as the knickpoints retreat over the course of the experiments (up to 150 minutes) rather than interpreting such change in the natural environment. Here, we exploit this experimental capability to explore the processes that drive the difference in channel geometry at and around knickpoints compared to equilibrium conditions.

Figure 3 shows the temporal evolution of the distribution of Width Ratios (WR), defined as the channel width divided by the equilibrium width, for all channel cross sections (excluding the upper and lower 10 cm of the channel). A WR of 1 implies that the channel is at equilibrium conditions whereas a $WR < 1$ is a channel that is narrower than equilibrium. All experiments, experience the same overall pattern of

channel narrowing, and then widening, as the geometry experiences the transient adjustment of the knickpoint propagating upstream from the outlet to the inlet (Fig. 3). Importantly, the narrowing of the channel caused by the knickpoint is not limited to the specific location of the knickpoint, with the dynamic width adjustment experienced along the full channel reach, although the focus of the greatest narrowing (smallest value of WR) typically follows the location of the knickpoint for all Q and Q_s combinations (see the relative position of the blue knickpoint line and the shaded pdf in Fig. 3). After the knickpoint has reached the channel inlet (vertical dashed blue line in Fig. 3), the WR typically continues to increase as the channel continues to re-adjust back towards equilibrium conditions and there is a shift from transport-limited to supply-limited conditions during knickpoint retreat.

2.2.2.2 Dynamic channel geometry evolution at a point location

By focussing on the evolution of the channel width and the vertical incision at a single location through time (Fig. 4), we can consider the complete response to the transient phase of incision driven by the propagation of the knickpoint. The substitution of space for time allows the rate of width adjustment before, during, and after knickpoint propagation to be extracted for the different experimental input conditions (Q and Q_s). The presence of the knickpoint at the channel mid-point coincides with the highest rates of vertical bed incision as well as the narrowest channel widths (Fig. 4). For a given Q , the WR at the knickpoint is smaller for the experiments with $Q_s = 0.00666 \text{ g cm}^{-3}$ than with $Q_s = 0 \text{ g cm}^{-3}$ (Fig. 4), implying a greater narrowing effect for channels that contain additional input sediment (also seen in Fig. 2).

The sharpest change in the vertical bed incision is associated with knickpoints that are present at the channel mid-point for a short duration (i.e., vertical steps undergoing parallel retreat; Fig. 4B; D; G; H) compared to more sustained, slower, periods of bed elevation change for longer duration knickpoints (typically steepened reaches; Fig. 4E; I). For the majority of the time during the experiments, the channels experience little bed elevation or channel width adjustment shown by the cluster of points near the origin of Figure 5. Importantly, where the rates of change of width (dW/dt) and bed elevation (dZ/dt) are furthest from zero, there is a trend in the overall vector direction of two-dimensional channel geometry change apparent in the

kernel density plots (Fig. 5B; D). The pattern of channel narrowing occurring when the bed is incising and channel widening occurring when the bed is aggrading is particularly evident when $Q_s = 0.00666 \text{ g cm}^{-3}$ (Fig. 5C; D). We can identify three phases of channel response at a point location during the passage of the transient knickpoint (Fig. 4): (1) the channel narrows as the knickpoint approaches, coincident with the beginning of an increase in vertical incision rate and local steepening of the channel, (2) the knickpoint propagates past the point-location, with heightened vertical incision and the narrowest widths, followed by (3) channel widening immediately after the knickpoint has propagated past with limited incision or sediment aggradation on the bed during the widening phase (Fig. 4). The mean duration of channel narrowing until the narrowest recorded width at the channel mid-point (40 cm from the outlet) was 48 minutes after the start of the experiment. Channel widening at the channel mid-point following the passage of the knickpoint continued until the end of the experiment (average from time of recorded width until end of experiment = 68 minutes), including during the period after the knickpoint had retreated the full reach length to the channel inlet (e.g., Fig. 4A;H).

3. Discussion

The experimental results presented here demonstrate a clear link between channel width variability and the retreat of knickpoints within bedrock channels. Here, we discuss the drivers of channel change at knickpoints (section 3.1), the implications for adjoining hillslopes (section 3.2), insights into the response time of landscapes (section 3.3) and finally the role of sediment and the role of sediment (section 3.4).

3.1 Drivers of channel change at knickpoints

The systematic narrowing of bedrock channels associated with high tectonic uplift rate, active faulting or landslide dams has been observed in the natural environment (e.g., Burbank et al., 1996; Duvall et al., 2004; Whittaker et al., 2007; Ouimet et al., 2008; Cook et al., 2013), or within numerical model outputs (e.g., Yanites, 2018) and is thought to be associated with an intrinsic mechanism induced by high local slope that leads to focussed flow, high shear stresses and stream power, bedrock scour and a narrower channel with a smaller width-depth ratio (Finnegan et al., 2005; Whittaker et al., 2007). The rapid headward retreat of a knickpoint in the Da'an river, Taiwan (Cook et al., 2013; 2014; 2020) is the most relevant natural analogue for the

experimental results presented here due to the discrete generation of a single knickpoint following the uplift of an anticline feature during the 1999 Chi-Chi earthquake. Cook et al. (2013) documented the controls on the rapid retreat knickpoint rate and subsequent channel geometry adjustment at the reach scale, although the magnitude and pattern of channel narrowing and widening was not the main focus of their work. Before the Chi-Chi earthquake, the Da'an river flowed across a ~450 m wide braidplain (W_{Eq}) over the anticline and the initial knickpoint retreat cut an incised gorge 14 m deep (KP_H) and 31 m wide (W_{KP}), 7% of the pre-disturbance width (Cook et al., 2013). Following the rapid passage of the knickpoint past a point (> 100 m per year between 2004 and 2008), the channel width widened initially at 5 m per year (2005-2008) before slowing to 1.5 m per year (2008-2013).

In these experiments, we demonstrate the same phenomenon of channel narrowing and widening as observed in the Da'an river by Cook et al. (2013), demonstrating the relevance of our results for natural channels. Significant channel narrowing (up to 10% of equilibrium width; a similar order of magnitude to the Da'an river) occurs as part of the migration process of a specific knickpoint in the experiments, triggered by an instantaneous base level fall and generation of a vertical step at the channel outlet. The vertical step commonly diffuses into an oversteepened reach knickpoint with a downstream scour/plunge pool over a distance of up to five channel widths as it migrates upstream (Fig. 1), with an associated pulse of narrowing where channels can be as little as 10% of the width at equilibrium conditions (Fig. 2). The narrower, and steeper, channels lead to bed shear stress values $> 100\%$ higher immediately upstream of the knickpoint compared to equilibrium conditions. The power law exponent, b , ($W = KQ^b$) between channel width and discharge (or drainage area) is similar for equilibrium channels as well as knickpoints ($b \sim 0.5$), matching the findings of Duvall et al., (2004). However, the value of K is approximately three times smaller for the knickpoints (Fig. 2), showing the importance of reach-scale variability in response to transient forcing (instantaneous base level fall) on the channel width. Similar to the observations in the Da'an river, the rate of channel widening following knickpoint retreat is prolonged compared to the shorter duration of narrowing as the knickpoint approaches the point location (Fig. 4)

At a single location during a transient response of a bedrock reach to base level fall, channel geometry adjustment is characterised by long periods of slow and gradual

adjustment punctuated by a short pulse of vertical incision, demonstrated by the cluster of data where both dW/dt and dZ/dt are near zero with fewer points where $dZ/dt \ll 0$ in Fig. 5. Furthermore, the vector direction of channel geometry adjustment matches observations in the field of channel widening occurring during phases of aggradation (e.g., East et al., 2015) and channel narrowing during incision (e.g., Finnegan et al., 2007; Johnson et al., 2010), highlighting the importance of understanding the role of dynamic river width when considering bedrock river adjustment to external forcing.

According to hydraulic theory associated with the acceleration zone upstream of a knickpoint lip (e.g., Rouse, 1936), some of the increase in bed shear stress may be induced by the change from hydrostatic pressure to atmospheric pressure (equation 1). We find that this hydraulic theory can only account for a small fraction of the total increase in bed shear stress observed in the experiments (Fig. 6A), and the residual bed shear stress appears to be related to the magnitude of channel width narrowing (Fig. 6B; correlation coefficient = 0.52). The hydraulic theory associated with the zone of flow acceleration upstream of the knickpoint lip suggests that any impact is experienced over an along-stream distance of a few water depths (Haviv et al., 2006). The experimental results here (e.g., Fig. 3) show that the whole mechanism of transient width variation can impact a reach of distance $>$ five channel widths and any purely hydraulic-induced width variability component is relatively minimal overall.

Following the instantaneous base level fall, the transient response of the channel acts to return the channel back to the smooth profile representative of equilibrium conditions. In the experiments, where the substrate can be eroded through clear water flow, the channel width self-forms in order to optimise the bed shear stress for producing the most efficient upstream propagation of the knickpoint by eroding and transport the bed material until the downstream reach that is graded to the new outlet elevation. The width-adjustment process to optimise the bed shear stress follows the width-adjustment model proposed by Yanites (2018), where a channel will tend towards a condition that leads to the greatest vertical incision.

We can speculate that the excess higher shear stress observed beyond what is predicted by the hydraulic theory of the acceleration zone is due to the requirement for the channel to increase its transport capacity and bed shear stress in order to

transport the optimum material eroded from the knickpoint in addition to the sediment supplied from upstream in the most efficient way possible. Narrowing of channels in order to increase the transport capacity has been numerically modelled suggested for the mobilisation of landslide material following a sudden input of sediment (Croissant et al., 2017), and we suggest a similar mechanism is occurring during knickpoint retreat. The hydraulic theory of Rouse (1936) does not take into account knickpoint generation and longer-term shift of a channel from equilibrium conditions. Rather it predicts the hydraulics at knickpoints themselves, so it could be expected that any hydraulic-induced width variability is superimposed on the more significant transport capacity-induced width variability.

The set of experiments that included an additional input of coarse sediment had a higher bed shear stress both at equilibrium and knickpoint conditions (Fig. 2C), driven by the requirement to transport both the eroded material from the knickpoint as well as the sediment load from upstream. There is a larger difference between τ_{Eq} and τ_{KP} than between the $Q_s = 0 \text{ g cm}^{-3}$ and $Q_s = 0.00666 \text{ g cm}^{-3}$ experiments, highlighting that in the cases tested here, the transient nature of channels is more significant for their geometry than variability in upstream sediment supply.

3.2 Hillslope-channel coupling

The impact of headward knickpoint migration on adjoining hillslopes through the vertical reduction of the hillslope 'base level' elevation can be significant in triggering the onset of active hillslope processes downstream of the knickpoints (e.g., Reinhardt et al., 2007; Gallen et al. 2011). The phases of lateral channel adjustment associated with knickpoint retreated highlighted in the experiments presented here (narrowing then widening) highlights an additional mechanism for the destabilisation of the adjoining hillslopes. As the channel geometry relaxes back to equilibrium conditions following the knickpoint migration, the width can increase by more than 50% (and up to 80% where channels have a high sediment load; Figure 2). Channel widening through bank erosion or gorge wall retreat has been shown to destabilise hillslopes through undermining of the hillslope toe (Harvey, 2001; Kondolf et al., 2002; Golly et al., 2017), and steepening of the hillslope beyond the threshold angle for failure (Larsen and Montgomery, 2012), so it would be anticipated that knickpoint retreat can drive hillslope destabilisation by both the rapid vertical incision as well as

the lateral adjustment component. To assess the relative importance of vertical channel incision (defined as the knickpoint height, KP_H) and lateral adjustment component (defined as $W_{Eq} - W_{KP}$) on hillslope destabilisation, we calculated the ratio $\frac{KP_H}{(W_{Eq} - W_{KP})\tan\theta}$ where θ is the hillslope angle. In Figure 7, we used a hillslope angle of 30° , a value appropriate for representing hillslopes at a typical angle of repose (e.g., Whittaker et al., 2007) and identified the experiments where

$\frac{KP_H}{(W_{Eq} - W_{KP})\tan\theta} < 1$ to indicate when the lateral widening component is more important

for hillslope destabilisation than the magnitude of the channel incision (i.e., the knickpoint height). The lateral adjustment process is relatively more important than vertical incision for hillslope destabilisation in the experiments with higher Q (Fig. 7A).

We suggest this is due to the lower values of $\frac{KP_H}{W_{Eq}}$ at higher Q , when KP_H is fixed

across all experiments (Fig. 7B). This equation could also be applied in natural field settings where knickpoint width, knickpoint height, hillslope angle and equilibrium channel width can be estimated, and we can suggest that hillslope destabilisation

driven by lateral channel undercutting can be particularly prevalent in circumstances where the channel width is relatively large compared to the knickpoint height (when

$\frac{KP_H}{W_{Eq}} < \sim 0.7$).

The hillslope response to knickpoint migration can be mapped to the same three phases described above and shown conceptually in Figure 8: (1) Hillslopes become decoupled from the channel as the width narrows and there is an increase in the incision rate as the knickpoint approaches. (2) As the knickpoint propagates past the point-location, rapid vertical bed incision leads to rapid reduction in the hillslope base level that triggers hillslope destabilisation (Gallen et al. 2011; Mackey et al. 2014).

(3) Channel widening after the knickpoint has propagated past, leading to continued hillslope destabilisation. The wave of knickpoint-induced lateral adjustment can be an integral feature of the coupling of hillslopes and channels in transient landscapes, depending on the relative magnitudes of KP_H and W_{Eq} .

3.3 Landscape Response time

Figures 3&4 provide insight into the timescale of the wave of knickpoint-induced lateral adjustment of the channel geometry, with the channel widening continuing for

a prolonged period of time after the passage of the knickpoint. For example, the channel width at the channel mid-point is still increasing at the time that the knickpoint has reached the channel inlet 40 cm upstream for most of the experiments (Fig. 4). The range of W_{Eq} is from 4 to 10 cm (Fig. 3), suggesting that the lateral adjustment phase is at least the time taken for the knickpoint to retreat four to ten channel widths. In all experiments, the rate of lateral adjustment is slower than the rate of upstream knickpoint retreat (Fig. 4), such that the duration of the lateral adjustment phase is sustained over a significant longer period than the relatively rapid pulse of vertical incision associated with the passage of a knickpoint. Lateral erosion associated with channel widening downstream of a migrating knickpoint is therefore an important bottom-up control on hillslope stability leaving an ongoing legacy of knickpoint retreat within the landscape, and may erode evidence of past environmental conditions through the removal of preserved strath terraces downstream of knickpoints (Baynes et al., 2018b). The longer-term legacy of knickpoint retreat on hillslopes has important implications for setting the wider timescale of landscape response to transient forcing (Hurst et al., 2019) and variable channel width should be an important component of landscape evolution models where possible. The quantification of rates of channel widening relative to knickpoint retreat in natural settings would further demonstrate the importance of in-channel processes for hillslope destabilisation.

3.4.3 Role of in-channel sediment supply in setting the degree of hillslope destabilisation

Previous field and experimental observations (e.g., Baynes et al., 2020) and modelling studies (Turowski, 2018; 2020; Li et al., 2020) have shown that channels with higher sediment supplies are typically wider for a given discharge, thought to be due to the 'cover effect' that protects the bed from vertical incision and encourages lateral erosion of the banks by particle impacts (the 'tools effect'; Sklar and Dietrich, 2004). Here, we show that sediment rich channels under transport-limited conditions are not only wider under equilibrium conditions (Baynes et al., 2020), they also undergo a more dynamic response to transient forcing (i.e., knickpoint retreat), as they narrow proportionally more from their equilibrium state compared to low Q_s channels (Figs. 2; 4). Absolute KP_W values are similar for both $Q_s = 0$ and $0.00666 \text{ g cm}^{-3}$ experiments at a given discharge (Fig. 2A), which is expected as the higher

slope at the knickpoint increases the sediment transport capacity significantly (Croissant et al., 2017) such that the higher sediment supply has a negligible impact on the channel width under knickpoint conditions compared to equilibrium (Baynes et al., 2020). As the channels return to W_{Eq} following the passage of the knickpoint and the slope of the channel is reduced (during phase 3 in Fig. 8), channels with a high Q_s and therefore the bed is protected by the 'cover effect' widen to a larger extent and therefore potentially have a stronger role in undermining the adjoining hillslopes through bank erosion (Kondolf et al., 2001). There exists a potential positive feedback, whereby channels with a higher Q_s experience a more pronounced wave of lateral adjustment during knickpoint retreat, leading to an increased likelihood of hillslope destabilisation following the passage of a knickpoint. In turn, the heightened hillslope instability supplies more sediment to the channel through mass wasting (Gallen et al., 2011; Attal et al., 2015), completing the positive feedback loop with a wider equilibrium channel state before the migration of subsequent knickpoints in response to further base level falls. Such an observation from the experiments presented here, highlights an additional complexity resulting from the presence of sediment in bedrock channels and highlights its importance for both erosion processes and wider landscape response.

4. Conclusion

Headward migrating knickpoints are key features of transiently adjusting landscapes through the translation of bottom-up signals of base level fall or changes in tectonic uplift through the river network and the adjoining hillslopes. In addition to the rapid vertical incision associated with knickpoint passage, we show here using a suite of analogue flume experiments that a wave of lateral adjustment of channel geometry; narrowing by up to 80% compared to equilibrium conditions followed by a widening after the passage of a knickpoint, can have a long-lasting impact on the stabilisation of hillslopes. The relative degree of channel narrowing/widening is independent of the water discharge, but channels with a high sediment load experience a greater extent of narrowing/widening compared to channels with a lower sediment load, and the lateral adjustment can be more important for the destabilisation of hillslopes than the magnitude of vertical incision. Rates of lateral adjustment are typically slower than the rates of upstream knickpoint migration, therefore having a longer term impact on the stability of hillslopes than rapid bed elevation change. These

observations enhance the importance of understanding the key processes that drive the migration of knickpoints, as the localised channel geometry response has ongoing implications for the stability of adjoining hillslopes and, therefore, the supply of sediment to the channel network and export from landscapes.

References

- Attal, M., Mudd, S.M., Hurst, M.D., Weinman, B., Yoo, K., Naylor, M., (2015) Impact of change in erosion rate and landscape steepness on hillslope and fluvial sediments grain size in the Feather River basin (Sierra Nevada, California). *Earth Surface Dynamics* 3, 201-222
- Baynes, E.R.C., Lague, D., Attal, M., Gangloff, A., Kirstein, L.A., Dugmore, A.J., (2018a) River self-organisation inhibits discharge control on waterfall migration. *Scientific Reports* 8, 2444
- Baynes, E.R.C., Lague, D., Kermarrec, J-J., (2018b) Supercritical river terraces generated by hydraulic and geomorphic interactions. *Geology* 46 (6), 499-502
- Baynes, E.R.C., van de Lageweg, W.I., McLelland, S.J., Parsons, D.P., Aberle, J., Dijkstra, J., Henry, P-Y., Rice, S.P., Thom, M., Moulin, F., (2018c) Beyond equilibrium: re-evaluating physical modelling of fluvial systems to represent climate changes. *Earth-Science Reviews* 181, 82-97
- Baynes, E.R.C., Lague, D., Steer, P., Bonnet, S., Illien, L., (2020) Sediment flux-driven channel geometry adjustment of bedrock and mixed gravel-bedrock rivers. *Earth Surface Processes and Landforms* 45 (14), 3714-3731
- Bigi, A., Hasbargen, L.E., Montanari, A., Paola, C., (2006) Knickpoints and hillslope failures: Interactions in a steady-state experimental landscape. In: Willett, S.D., Hovius, N., Brandon, M.T., Fisher, D.M., (Eds) *Tectonics, Climate, and Landscape Evolution*. Geological Society of America, Boulder. 295-307
- Burbank, D.W., Leland, J., Fielding, E., Anderson, R.S., Brozovic, N., Reid, M.R., Duncan, C. (1996) Bedrock incision, rock uplift and threshold hillslopes in the northwestern Himalayas. *Nature* 379, 505-510

Cook, K.L., Turowski, J.M., Hovius, N. (2013) A demonstration of the importance of bedload transport for fluvial bedrock erosion and knickpoint propagation. *Earth Surface Processes and Landforms* 38, 683-395

Cook, K.L., Turowski, J.M., Hovius, N. (2014) River gorge eradication by downstream sweep erosion. *Nature Geoscience* 7 (9), 682-686

Cook, K.L., Turowski, J.M., Hovius, N. (2020) Width control on event-scale deposition and evacuation of sediment in bedrock-confined channels. *Earth Surface Processes and Landforms* 45, 3702-3713

Croissant, T., Lague, D., Steer, P., Davy, P. (2017) Rapid post-seismic landslide evacuation boosted by dynamic river width. *Nature Geoscience* 10, 680-684

Davy, P., Croissant, T., Lague, D., (2017) A precipitation method to calculate river hydrodynamics, with applications to flood prediction, landscape evolution models, and braiding instabilities. *Journal of Geophysical Research – Earth Surface* 122: 1491-1512

De Lavaissiere, L. Bonnet, S., Guyez, A., Davy, P. (2021) Generation of autogenic knickpoints in laboratory landscape experiments evolving under constant forcing. *Earth Surface Dynamics Discussions [preprint]*. <https://doi.org/10.5194/esurf-2021-50>

DiBiase, R., Whipple, K.X., Lamb, M.P., Heimsath, A.M., (2015) The role of waterfalls and knickzones in controlling the style and pace of landscape adjustment in the western San Gabriel Mountains, California. *Geological Society of America Bulletin* 127 (3-4): 539–559.

Duvall, A., Kirby, E., Burbank, D., (2004) Tectonic and lithologic controls on bedrock channel profiles and processes in coastal California. *Journal of Geophysical Research* 109, F03002.

East, A.E., Pess, G.R., Bountry, J.A., Magirl C.S., Ritchie, A.C., Logan, J.B., Randle, T.J., Mastin M.C., Minear J.T., Duda, J.J., Liermann, M.C., McHenry, M.L., Beechie, T.J., Shafroth, P.B. (2015) Reprint of: Large-scale dam removal on the Elwha River, Washington, USA: River channel and floodplain geomorphic change. *Geomorphology* 246, 687-708

Finnegan, N.J., Roe, G., Montgomery, D.R., Hallet, B. (2005) Controls on the channel width of rivers: Implications for modelling fluvial incision into bedrock. *Geology* 33 (3), 229-232

Finnegan, N.J., Sklar, L.S., Fuller, T.K., (2007) Interplay of sediment supply, river incision, and channel morphology revealed by the transient evolution of an experimental bedrock channel. *Journal of Geophysical Research* 112, F03S11

Flores-Cervantes, J.H., Istanbuluoglu, E., Bras, R.L., (2006) Development of gullies on the landscape: A model of headcut retreat resulting from plunge pool erosion. *Journal of Geophysical Research* 111, F01010.

Gallen, S.F., Wegmann, K.W., Frankel, K.L., Hughes, S., Lewis, R.Q., Lyons, N., Paris, P., Ross, K., Bauer, J.B., Witt, A.C., (2011) Hillslope response to knickpoint migration in the Southern Appalachians: implications for the evolution of post-orogenic landscapes. *Earth Surface Processes and Landforms* 36, 1254-1267

Gardner, T., (1983) Experimental study of knickpoint and longitudinal profile evolution in cohesive, homogenous, material. *Geological Society of America Bulletin* 94, 664-672

Golly, A., Turowski, J.M., Badoux, A., Hovius, N., (2017) Controls and feedbacks in the coupling of mountain channels and hillslopes. *Geological Society of America Bulletin* 45 (4), 307-310.

Grieve, S.W.D., Mudd, S.M., Hurst, M.D., (2016) How long is a hillslope? *Earth Surface Processes and Landforms* 41 (8), 1039-1054

Groh, E.L., Scheingross, J.S., (2021) Morphologic signatures of autogenic waterfalls: A case study in the San Gabriel Mountains, California. *Geology*
<https://doi.org/10.1130/G49320.1>

Hasbergen, L., Paola, C., (2000) Landscape instability in an experimental drainage basin. *Geology* 28 (12), 1067-1070.

Harvey, A.M., (2001) Coupling between hillslopes and channels in upland fluvial systems: implications for landscape sensitivity, illustrated from the Howgill Fells, northwest England. *Catena* 42, 225-250

Haviv, I., Enzel, Y., Whipple, K.X., Zilberman, E., Stone, J., Matmon, A., Fifield, L.K., (2006) Amplified erosion above waterfalls and oversteepened bedrock reaches. *Journal of Geophysical Research* 111, F04004.

Hooke, R., (1968) Model Geology: prototype and laboratory streams: discussion. *Geological Society of America Bulletin* 79, 391-394

Hurst, M.D., Mudd, S.M., Attal, M., Hilley, G., (2013) Hillslopes record the growth and decay of landscapes. *Science* 341 (6148), 868-871

Hurst, M.D., Grieve, S.W.D., Clubb, F.J., Mudd, S.M., (2019) Detection of channel-hillslope coupling along a tectonic gradient. *Earth and Planetary Science Letters* 522, 30-39.

Johnson, J.P.L, Whipple, K.X., Sklar, L.S. (2010) Contrasting bedrock incision rates from snowmelt and flash floods in the Henry Mountains, Utah. *Geological Society of America Bulletin* 122 (9-10), 1600-1615

Kondolf, G.M., Piegay, H., Landon, N., (2002) Channel response to increased and decreased bedload supply from land use change: contrasts between two catchments. *Geomorphology* 45, 35-51

Korup, O., Schlunegger, F., (2007) Bedrock landsliding, river incision, and transience of geomorphic hillslope-channel coupling: Evidence from inner gorges in the Swiss Alps. *Journal of Geophysical Research* 112, F03027

Lague, D., (2014) The stream power incision model: evidence, theory and beyond. *Earth Surface Processes and Landforms* 39 (1), 38-61

Lapotre, M.G.A., Lamb, M.P., (2015) Hydraulics of floods upstream of horseshoe canyons and waterfalls. *Journal of Geophysical Research: Earth Surface* 120, 1227-1250

Larsen, I.J., Montgomery, D.R., (2012) Landslide erosion coupled to tectonics and river incision. *Nature Geoscience* 5, 468-473

Li, T., Fuller, T.K., Sklar, L.S., Gran, K.B., Venditti, J.G., (2020) A mechanistic model for lateral erosion of bedrock channel banks by bedload particle impacts. *Journal of Geophysical Research: Earth Surface* 125 (6), e2019JF005509

Mackey, B.H., Scheingross, J.S., Lamb, M.P., Farley, K.A., (2014) Knickpoint formation, rapid propagation, and landscape response following coastal cliff retreat at the last interglacial sea-level highstand: Kaua'i, Hawai'i. *Geological Society of America Bulletin* 126 (7-8), 925-942

Ouimet, W.B., Whipple, K.X., Crosby, B.T., Johnson, J.P., Schildgen, T.F. (2008) Epigenetic gorges in fluvial landscapes. *Earth Surface Processes and Landforms* 33, 1993-2009

Paola, C., Straub, K.M., Mohrig, D.C., Reinhardt, L., (2009) The "unreasonable effectiveness" of stratigraphic and geomorphic experiments. *Earth Science Reviews* 97, 1-43

Reinhardt, L.J., Bishop, P., Hoey, T.B., Dempster, T.J., Sanderson, D.C.W. (2007) Quantification of the transient response to base-level fall in a small mountain catchment. Sierra Nevada, southern Spain. *Journal of Geophysical Research* 112, F03S05

Rouse, H. (1936) Discharge characteristics of the free overfall. *Civil Engineering*, 6 (4), 257-260.

Sklar, L.S., Dietrich, W.E., (2004) A mechanistic model for river incision into bedrock by saltating bed load. *Water Resources Research*, 40, W06301

Stein, O.R., Julien, P.Y., (1993) Criterion delineating the mode of headcut migration. *Journal of Hydraulic Engineering* 119, 37-50.

Turowski, J.M., (2018) Alluvial cover controlling the width, slope and sinuosity of bedrock channels. *Earth Surface Dynamics* 6, 29-48

Turowski, J.M., (2020) Mass balance, grade, and adjustment timescales in bedrock channels. *Earth Surface Dynamics* 8, 103-122

Turowski, J.M., Lague, D., Hovius, N. (2009) Response of bedrock channel width to tectonic forcing: Insights from a numerical model, theoretical considerations, and comparison with field data. *Journal of Geophysical Research: Earth Surface* 114 (F3)

Valla, P., Van der Beek, P., Lague, D., (2010). Fluvial incision into bedrock: insights from morphometric analysis and numerical modelling of gorges incision glacial

hanging valleys (Western Alps, France). *Journal of Geophysical Research* 115, F02010

Whitbread, K., Jansen, J., Bishop, P., Attal, M., (2015) Substrate, sediment, and slope controls on bedrock channel geometry in postglacial streams. *Journal of Geophysical Research: Earth Surface* 120 (5), 779-798

Whittaker A.C., Boulton S.J., (2012) Tectonic and climatic controls on knickpoint retreat rates and landscape response times. *Journal of Geophysical Research* 117: F02024. DOI. 10.1029/2011JF002157

Whittaker, A.C., Cowie, P.A., Attal, M., Tucker, G.E., Roberts, G.P., (2007) Bedrock channel adjustment to tectonic forcing: implications for predicting river incision rates. *Geology* 25 (2), 103-106.

Wobus, C.W., Tucker, G.E., Anderson, R.S., (2006) Self-formed bedrock channels. *Geophysical Research Letters* 33, L18408

Yanites, B.J., Tucker, G.E., (2010) Controls and limits on bedrock channel geometry. *Journal of Geophysical Research* 115, F04019

Yanites, B.J. (2018) The Dynamics of Channel Slope, Width, and Sediment in Actively Eroding Bedrock Systems. *Journal of Geophysical Research* 123, 1504-1527

Table 1: Experiment input conditions

Experiment number	Water discharge (cm ³ s ⁻¹)	Input sediment flux (g cm ⁻³)
1	8.33	0
2	12.5	0
3	16.67	0
4	25	0
5	33.33	0
6	50	0
7	8.33	0.00666
8	16.67	0.00666
9	25	0.00666
10	33.33	0.00666
11	50	0.00666

Accepted Article

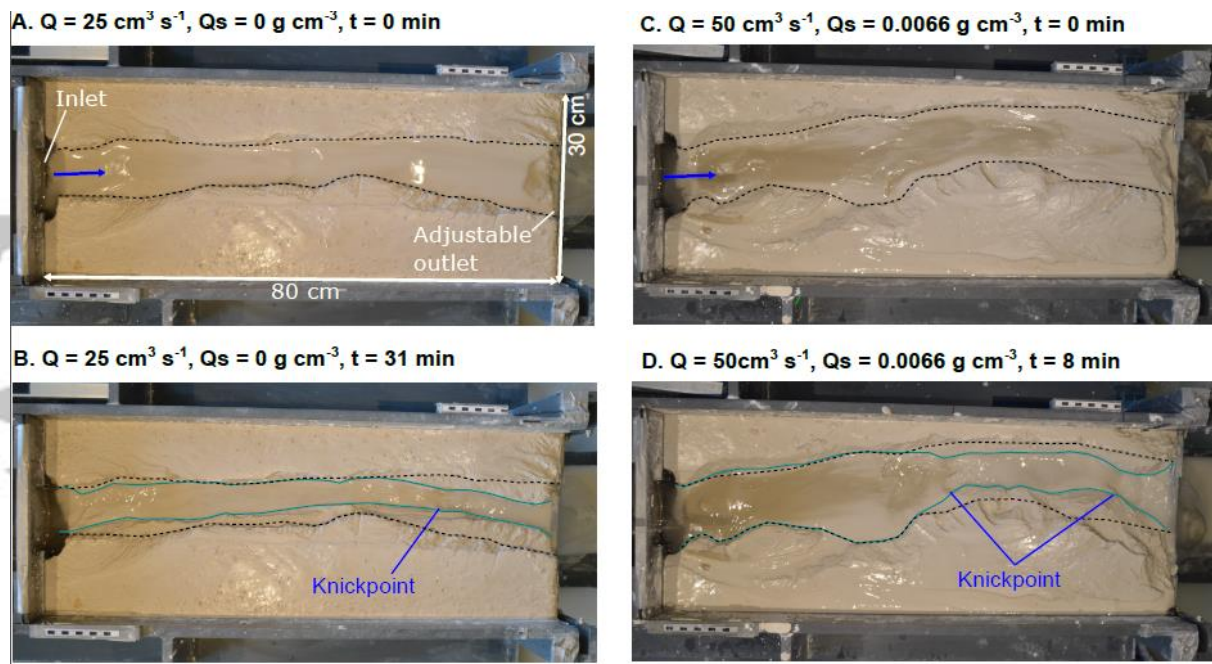


Figure 1: Photos from mounted camera above the Bedrock River Experimental Incision Tank, showing the experimental setup. Photos on the top show the equilibrium channel conditions at the start of an experiment where $Q_s = 0 \text{ g cm}^{-3}$ (A) and $Q_s = 0.00666 \text{ g cm}^{-3}$ (C), and photos on the bottom row (B and D) show the same channels containing knickpoints generated by an instantaneous dropping of the channel outlet. Black dashed lines show the limits of the channel at equilibrium conditions (A and C), and green solid lines show the channel limits in photos B and D for comparison.

Accepted

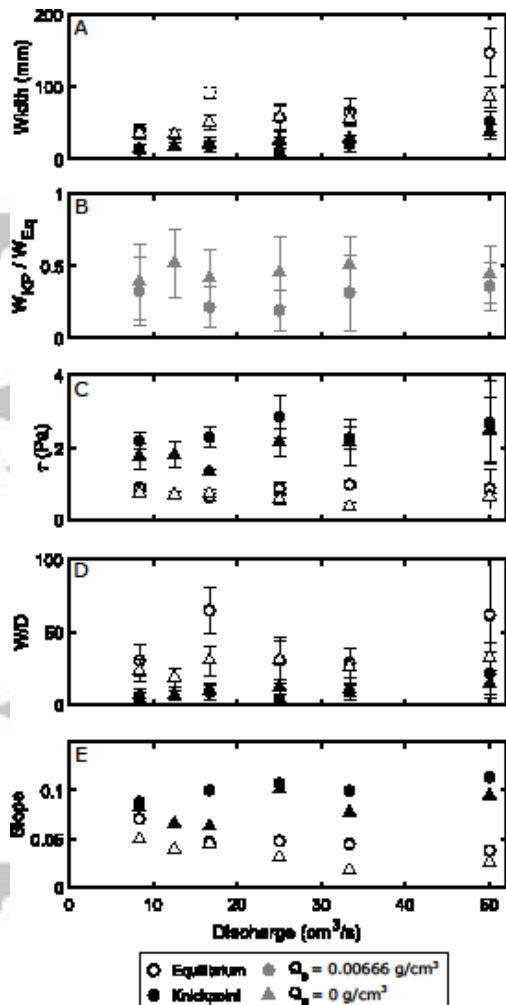


Figure 2: A: Channel width during equilibrium conditions (white) and at the knickpoints (black) plotted against discharge. Mean values are plotted with error bars indicating two standard deviations. Circles are experiments with $Q_s = 0 \text{ g cm}^{-3}$ and triangles are experiments with $Q_s = 0.00666 \text{ g cm}^{-3}$. B: The ratio of the knickpoint width to equilibrium channel width. C: Mean bed shear stress against discharge for both equilibrium conditions (white) and at the upstream lip of the knickpoints (black). Errorbars indicate two standard deviations. D: The width-depth ratio for both equilibrium conditions and at the knickpoint lip. E: The mean bed slope at equilibrium conditions (white) and the reach upstream of the knickpoint (black).

Figure 2: A: Channel width during equilibrium conditions (white) and at the knickpoints (black) plotted against discharge. Mean values are plotted with error bars indicating two standard deviations. Circles are experiments with $Q_s = 0 \text{ g cm}^{-3}$ and triangles are experiments with $Q_s = 0.00666 \text{ g cm}^{-3}$. B: The ratio of the knickpoint width to equilibrium channel width. C: Mean bed shear stress against discharge for both equilibrium conditions (white) and at the upstream lip of the knickpoints (black). Errorbars indicate two standard deviations. D: The width-depth ratio for both equilibrium conditions and at the knickpoint lip. E: The mean bed slope at equilibrium conditions (white) and the reach upstream of the knickpoint (black).

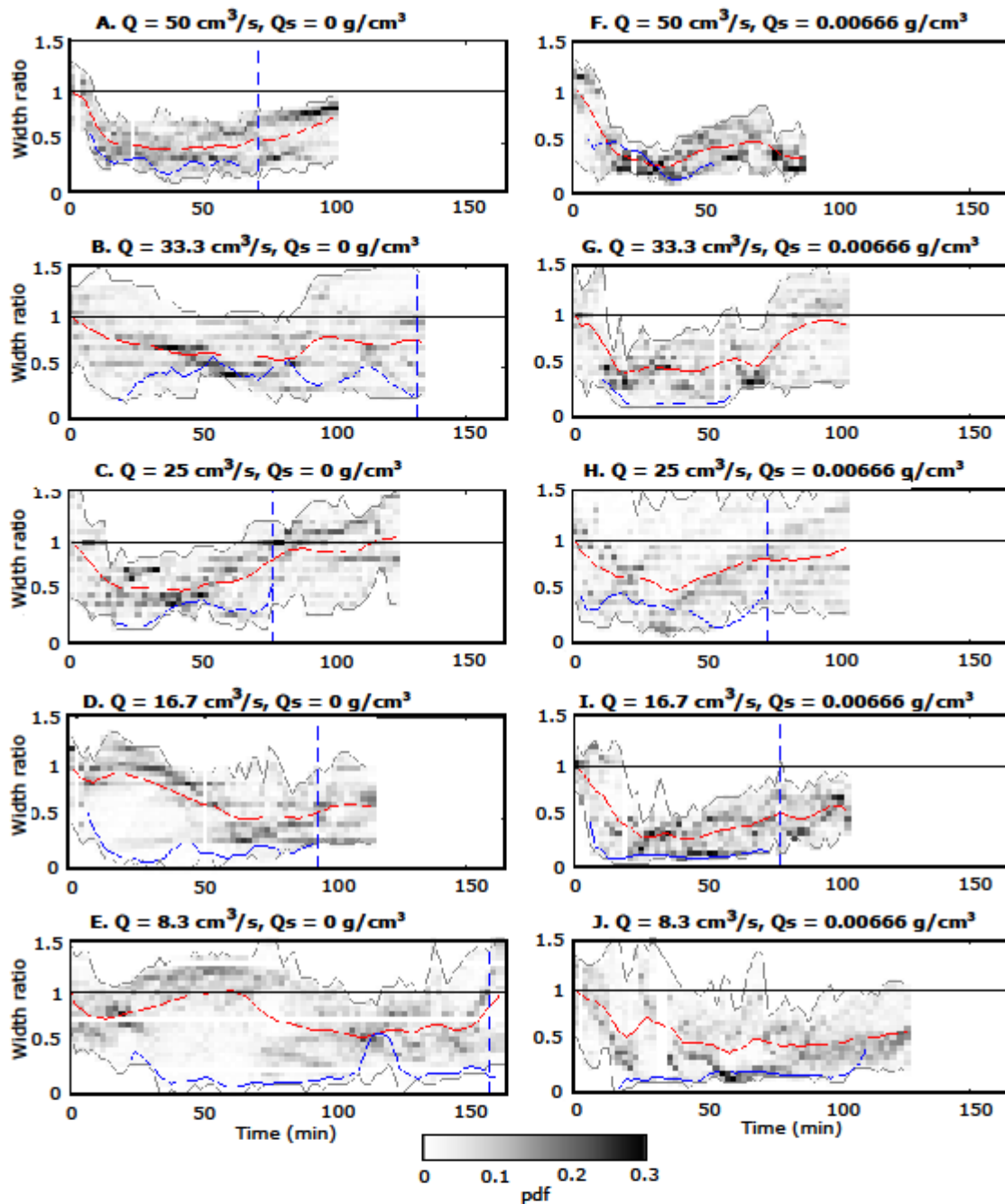


Figure 3: Evolution of width ratio (channel width/equilibrium width) through time for all channel cross-sections, excluding the upper and lower 10 cm to avoid inlet/outlet effects. For each time step, the red line is the mean width ratio across all the channel cross-sections, the grey lines show the maximum and minimum width ratio for the channel cross-sections and the blue line is the width ratio at the cross-section identified as being the location of the knickpoint. Vertical blue dashed line shows the time when the knickpoint reached the channel inlet. Shaded grey shows the histogram (pdf) of width ratios across the length of the channel for each time step. Darker grey = higher proportion of the cross-sections at that time step have that width ratio value. Lighter grey = lower proportion of the cross-sections at that time step have that width ratio value. Left panels (A-E) are experiments when $Q_s = 0 \text{ g/cm}^3$ and right panels (F-J) are for when $Q_s = 0.00666 \text{ g/cm}^3$.

Figure 3: Evolution of width ratio (channel width/equilibrium width) through time for all channel cross-sections, excluding the upper and lower 10 cm to avoid inlet/outlet effects. For each time step, the red line is the mean width ratio across all the channel cross-sections, the grey lines show the maximum and minimum width ratio for the channel cross-sections and the blue line is the width ratio at the cross-section identified as being the location of the knickpoint. Vertical blue dashed line shows the time when the knickpoint reached the channel inlet. Shaded grey shows the histogram (pdf) of width ratios across the length of the channel for each time step. Darker grey = higher proportion of the cross-sections at that time step have that width ratio value. Lighter grey = lower proportion of the cross-sections at that time step have that width ratio value. Left panels (A-E) are experiments when $Q_s = 0 \text{ g cm}^{-3}$ and right panels (F-J) are for when $Q_s = 0.00666 \text{ g cm}^{-3}$.

Accepted Article

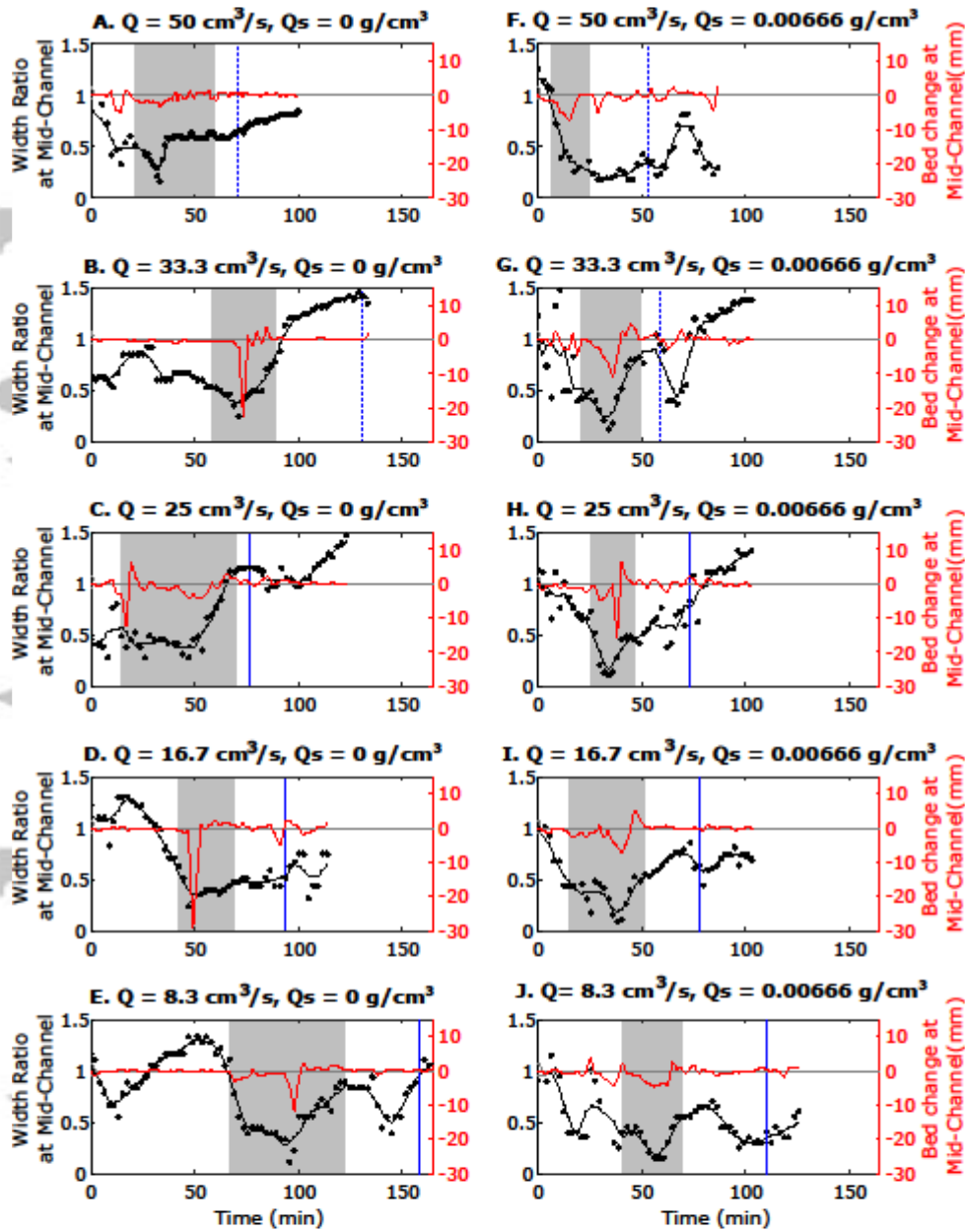


Figure 4: Analysis for the evolution of the width ratio and channel incision for the channel mid-point (50% distance from inlet to outlet) through time. Black points show the value of the width ratio, with the black line a five-point moving mean. Red line shows the channel incision at the mid-point through time calculated as the difference between the minimum bed elevation for the timestep and the minimum bed elevation at the preceding timestep. Shaded grey area show the time period when the knickpoint is present at the channel mid-point (i.e., time between steepened reach upstream of the knickpoint first reaching the mid-point and downstream limit of the pool migrating past the mid-point). Vertical blue dashed line indicates time when knickpoint reached the channel inlet.

Figure 4: Analysis for the evolution of the width ratio and channel incision for the channel mid-point (50% distance from inlet to outlet) through time. Black points show

the value of the width ratio, with the black line a five-point moving mean. Red line shows the channel incision at the mid-point through time calculated as the difference between the minimum bed elevation for the timestep and the minimum bed elevation at the preceding timestep. Shaded grey area show the time period when the knickpoint is present at the channel mid-point (i.e., time between steepened reach upstream of the knickpoint first reaching the mid-point and downstream limit of the pool migrating past the mid-point). Vertical blue dashed line indicates time when knickpoint reached the channel inlet.

Accepted Article

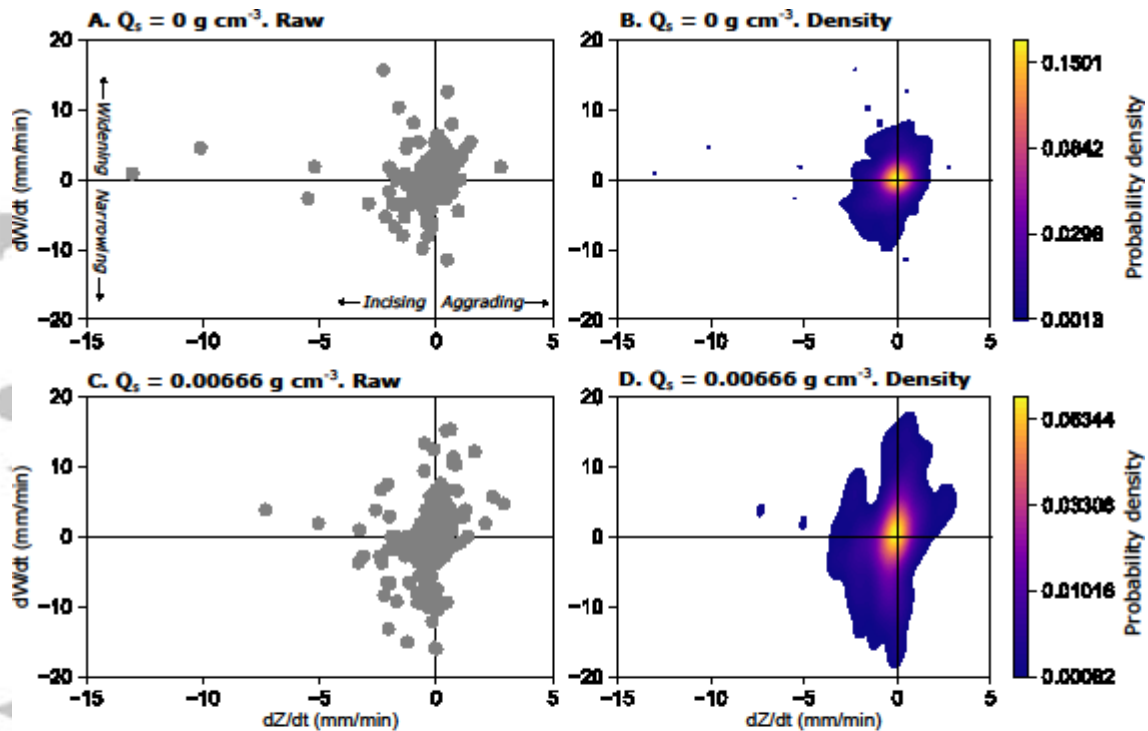


Figure 5: Combined data for the rate of change of channel width (dW/dt) as a function of rate of bed elevation change (dZ/dt) for all experiments where $Q_s = 0 \text{ g cm}^{-3}$ (A and B) and where $Q_s = 0.00666 \text{ g cm}^{-3}$ (C and D). B and D are kernel density plots of the raw data (A and C). Quadrants of each plot indicate where channels are widening ($dW/dt > 0$), narrowing ($dW/dt < 0$), aggrading ($dZ/dt > 0$) and narrowing ($dZ/dt < 0$).

Figure 5: Combined data for the rate of change of channel width (dW/dt) as a function of rate of bed elevation change (dZ/dt) for all experiments where $Q_s = 0 \text{ g cm}^{-3}$ (A and B) and where $Q_s = 0.00666 \text{ g cm}^{-3}$ (C and D). B and D are kernel density plots of the raw data (A and C). Quadrants of each plot indicate where channels are widening ($dW/dt > 0$), narrowing ($dW/dt < 0$), aggrading ($dZ/dt > 0$) and narrowing ($dZ/dt < 0$).

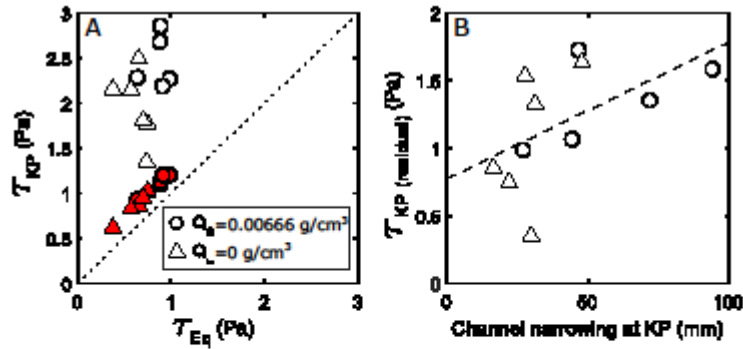


Figure 6: A: Shear stress at knickpoint lip against the shear stress under equilibrium conditions. White symbols indicate the observed shear stress, and the red symbols indicate the shear stress at the knickpoint lip predicted according to equation 1, induced by the flow acceleration zone upstream of the waterfall. Dotted line indicates $\tau_{Eq} = \tau_{KP}$. B: The knickpoint lip shear stress residual (observed – predicted) against the extent to which the channel narrowed during the transient knickpoint migration. Dashed line is a linear trend line with $R^2 = 0.27$ and correlation coefficient = 0.52.

Figure 6: A: Shear stress at knickpoint lip against the shear stress under equilibrium conditions. White symbols indicate the observed shear stress, and the red symbols indicate the shear stress at the knickpoint lip predicted according to equation 1, induced by the flow acceleration zone upstream of the waterfall. Dotted line indicates $\tau_{Eq} = \tau_{KP}$. B: The knickpoint lip shear stress residual (observed – predicted) against the extent to which the channel narrowed during the transient knickpoint migration. Dashed line is a linear trend line with $R^2 = 0.27$ and correlation coefficient = 0.52.

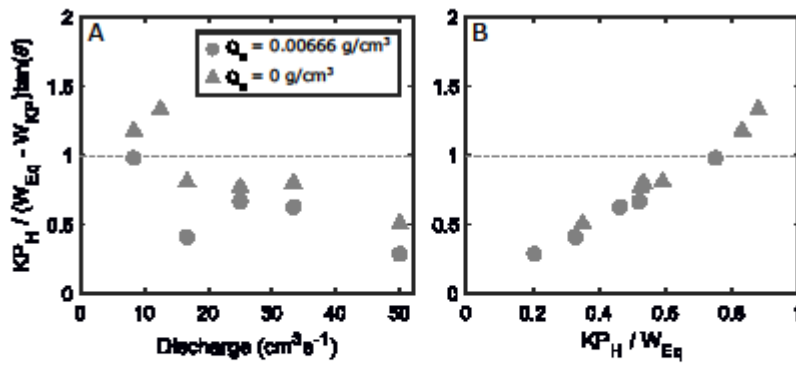


Figure 7: The relative importance of vertical incision by a knickpoint and lateral channel widening for the destabilisation of adjoining hillslopes, plotted against (A) flow discharge, and (B) the height of the knickpoint relative to the width of the equilibrium channel. Where $\frac{KP_H}{(W_{Eq} - W_{KP}) \tan \theta} < 1$, lateral channel widening is the more important component of hillslope destabilisation.

Figure 7: The relative importance of vertical incision by a knickpoint and lateral channel widening for the destabilisation of adjoining hillslopes, plotted against (A) flow discharge, and (B) the height of the knickpoint relative to the width of the equilibrium channel. Where $\frac{KP_H}{(W_{Eq} - W_{KP}) \tan \theta} < 1$, lateral channel widening is the more important component of hillslope destabilisation.

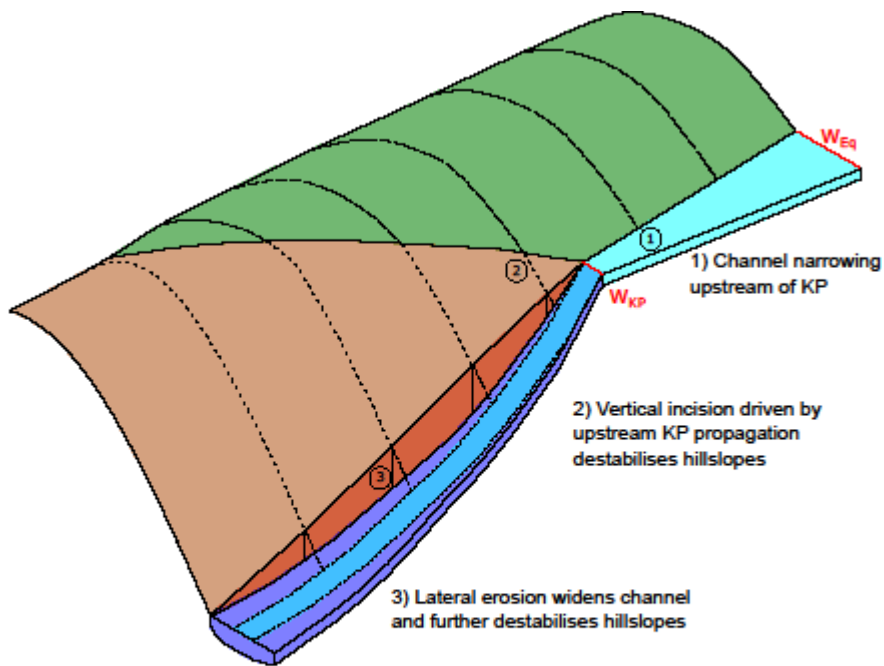


Figure 8: Conceptual diagram showing the phases of hillslope adjustment following channel evolution before (1), during (2) and after (3) the passage of a knickpoint past the hillslope toe. Adapted from Hurst et al. (2012) and Baynes et al. (2018a).

Figure 8: Conceptual diagram showing the phases of hillslope adjustment following channel evolution before (1), during (2) and after (3) the passage of a knickpoint past the hillslope toe. Adapted from Hurst et al. (2012) and Baynes et al. (2018a).

Accepted